Understanding vegetation variability and their "hotspots" within Lake Victoria Basin (LVB: 2003-2018)

B. Morgan[a], J.L. Awange[a,b], A. Saleem[a], & H. Kexiang[a]

[a] *School of Earth and Planetary, Spatial Science Discipline, Curtin University, Perth, Australia*

[b] *Geodetic Institute, Karlsruhe Institute of Technology, Engler-Strasse 7, D-76131, Karlsruhe, Germany*

Abstract

Lake Victoria's surface area has recently been shown to have shrunk by 0.3% compared to its 1984 value, a decline that has been associated with climatic as well as anthropogenic factors. Climatic factors include, e.g., reduced rainfall, which impacts not only on the lake's water level but also on the basin's vegetation that forms the lake's catchment. Understanding the locations of vegetation changes and the driving forces of such changes, therefore, is of most critical importance to major stakeholders regarding environmental management, policies and planning. For Lake Victoria Basin (LVB; Kenya, Uganda, Tanzania, Rwanda and Burundi), human development and climatic variability/change have subjected the region to significant changes in its vegetation characteristics whose spatio-temporal patterns are, however, not well understood. To understand this variability in vegetation for the period 2003-2018, this study employs the use of remotely sensed MODIS (Moderate Resolution Imaging Spectroradiometer), CHIRPS (Climate Hazards Group InfraRed Precipitation with station data) precipitation data, Google Earth Pro imagery, Gravity Recovery and Climate Experiment (GRACE)-based Mascon's total water storage (TWS) products and the statistical PCA (Principal Component Analysis). The study aims at determining (i) "significant hotspots", i.e. vegetation areas within the LVB largely impacted, and (ii), the extent of which anthropogenic and climatic variability have contributed to the "hotspots" formation. The results indicate a total of 8 hotspots; 5 in Uganda and 1 each in Kenya, Tanzania and Rwanda. Google Earth Pro imagery of all the hotspots show the changes in anthropogenic processes as the primary driver for the long-term changes in vegetation characteristics. Conversely, the analysis of PCA and Mascon's TWS concluded that only the Tanzanian hotspot may have been driven somewhat by climate variability. Climate variability is understood to be the driver in short-term vegetation changes while the long-term effects are driven primarily by human influence.

Keywords: CHIRPS; Lake Victoria; Vegetation change, NDVI; Climatic variability; Anthropogenic

1. Introduction

Studies have shown that alterations to the hydrological characteristics of freshwater areas correlate with changes in shoreline vegetation (e.g., (Hudon , 1997; Nilsson and Berggren , 2000; Baldwin et al., 2001; New and Xie , 2008)). Decreases in water-levels can allow vegetation types and other plant species the freedom to regenerate (Hill et al., 1998; Zhang et al., 2017). Conversely, anthropogenic processes that act to clear vegetation for urbanisation and development can indirectly lead to decreased water-levels of freshwater bodies that lie in proximity to where such stressors occur (Sand-Jensen et al., 2000; Zhang et al., 2017). Such water bodies provide important socio-economic services for the regions in which they are located, hence why they are sourced for extraction. For example, Jeppesen et al. (2012); Zhang et al. (2017); Sand-Jensen et al. (2000) investigate the extent of decline of flora species macrophyte around streams that are in close proximity to cultivated and urbanised regions and conclude that there are significant overall decrease of species richness for each of the streams they surveyed. Yet the converse is also true; anthropogenic activities such as use of fertilizers and industrial wastes also indirectly fuel increase in microphytes as demonstrated by Coladello et al., (2020) who studied macrophytes' abundance changes in eutrophicated tropical reservoir of Salto Grande in Brazil.

For the Lake Victoria Basin (LVB; 31°39' - 34°53' E and 0°20' - 3° N) that houses the second largest freshwater lake in the world (Mati et al., 2008), Awange et al. (2019a) employed medium-resolution remotely sensed data of Landsat (5, 7 & 8) and Sentinel-2 images for the period 1984-2018 and indicated that the surface area of the lake had shrunk significantly in recent decades at a rate of 5.97 km^2/year (from manual digitisation) and 5.27 km^2/year (from Modification of Normalized Difference Water Index (MNDWI)). Four areas that were identified as "hotspots", which had major influences in the overall reduction of Lake Victoria's surface area, i.e., Birinzi, Uganda - 33.9 km^2; Mwanza Gulf, Tanzania - 21.5 km^2; Emin Pasha Gulf, Tanzania - 14.6 km^2; and Winam Gulf, Kenya - 12.8 km^2 (Awange et al., 2019a).

To understand this decline, monitoring of its vegetational changes is vital and this predisposes it to remote sensing techniques due to its sheer size. This is because in-situ recordings over such a large area is impractical and extremely susceptible to inaccuracy, whilst photogrammetric processes would prove to be far too expensive when conducted yearly (Awange et al., 2019a). Even with this realization, there is little information pertaining to the changes in areal extent of LVB's vegetation coverage and their triggers. Studies that have been conducted have focussed largely on variance of NDVI values in the region (e.g., (Omute et al., 2012)) but have not equated the extent of which this contributes to changes in vegetation coverage. For instance, a 2014 study conducted in the Winam Gulf (Kenyan section of LVB) utilised coarse resolution 300 m MERIS (Medium Resolution Imaging Spectrometer) and fine resolution 30 m Landsat-7 imagery to analyse the NDVI of aquatic vegetation in the area, and performed accuracy assessments for each Normalised Difference Vegetation Index (NDVI) extraction method (Cheruiyot et al., 2014). With the gradual decrease in the surface area of Lake Victoria (Awange et al., 2019a), there is reason to suggest that this would be a driving force for changes in the characteristics of the surrounding vegetation within the catchment.

Factors that have been known to influence vegetation variability include both climatic and anthropogenic. For example, an NDVI variability study in the USA from 1982 - 1992 confirmed with a 99% confidence that El Ñino Southern Oscillation (ENSO) was the primary driver for influencing NDVI interannual variability (Li & Kafatos, 2000). A South African study (Richard & Poccard, 1998) found that seasonal rainfall changes were primary NDVI drivers in areas where the annual rainfall was between 300 and 900 mm, or if the total rainfall between the rainy and dry seasons were profound. Within LVB, Nicholson et al. (1990) and Omute et al. (2012) showed the influence of climate on vegetation by looking at the relationship between vegetation and rainfall in the region. Furthermore, climate variability through global teleconnections such as ENSO and Indian Ocean Dipole (IOD) on the one hand, and seasonal trends on the other hand, are also known influencers of short-term variability of vegetation in the LVB region (see e.g., Park et al., 2020; Zhao et al., 2020; Detsch et al., 2016; Williams & Hanan, 2011; Plisnier et al., 2000(@; Agutu et al., 2020; Omute et al., 2012; Awange et al., 2019a).

This study extends the work of Awange et al. (2019a), which analysed the physical dynamics of Lake Victoria by studying vegetation changes in its entire basin (i.e., LVB), which forms its catchment. The difference between the two studies is that Awange et al. (2019a) aimed at looking at changes on the physical surface of the lake and the triggers therein from 1984 to 2018. The current study employs high temporal-resolution MODIS (Moderate Resolution Imaging Spectroradiometer), CHIRPS (Climate Hazards Group InfraRed Precipitation with

Station) precipitation, Google Earth Pro imagery and Gravity Recovery and Climate Experiment (GRACE)-based Mascon's total water storage products for the 2003-2018 period, and the statistical PCA (principal component analysis), to determine (i) significant "hotspots", i.e., the main differences vegetation areas, which negatively impacted within LVB, and (ii), the extent of which anthropogenic and climatic variability have contributed to the "hotspots" formation. In undertaking this study, we seek to understand vegetational changes within LVB, which as catchment, is associated with the Lake's physical surface changes. Investigating the actual causality however, is out of the scope of the current work.

The remainder of the study is organised as follows: In Section 2, study area, the data and methods are presented. Section 3 covers results and discussion before concluding in Section 4.

2. Data and methods

2.1. Lake Victoria Basin: Background

Lake Victoria, the world's largest tropical lake and second-largest freshwater lake is located in Eastern Africa (31°39' - 34°53' E and 0°20' - 3° N), with its shoreline covering three countries, Kenya (6%), Uganda (45%) and Tanzania (49%) (Awange and Ong'ang'a , 2005; Mati et al., 2008). Its basin area (Figure 1) is almost three times the size of the lake and extends over the three East African countries together with Rwanda and Burundi. The basin refers to the network of rivers and streams that transport water and nutrients into the lake and is about 193000 km^2 (Awange and Ong'ang'a , 2005; Awange et al., 2008; Mati et al., 2008). It therefore facilitates the livelihood and wellbeing of over 40 million people across 5 countries at a density of over 300 people per km^2, with this population expecting to triple by the year 2050 (Awange et al., 2019a,b; Okotto-Okotto et al., 2018). Water levels for Lake Victoria are primarily dependent on rainfall (approx. 80% of total recharge) (Awange and Ong'ang'a , 2005; Awange et al., 2019a; Kizza et al., 2009). The remaining 20% is the result of discharge from within the catchment area (Awange and Ong'ang'a , 2005; Awange et al., 2008).

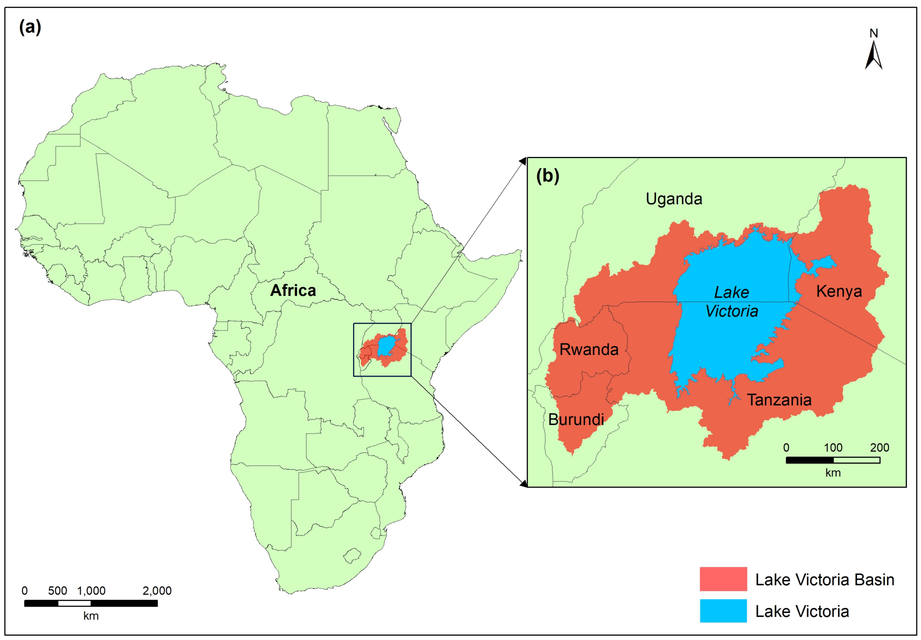

Figure 1: Lake Victoria Basin (LVB), the study area.

2.2. *Data*

Atmospherically corrected satellite images and hydroclimate data are employed to analyse the degree of which climate variability and anthropogenic activities has impacted on vegetation changes in the LVB. The data used for the investigation is elaborated upon in Sections 2.2.1–2.2.4 and summarized in Table 1.

2.2.1. *MODIS*

MODIS NDVI data products (eMODIS NDVI V6) are available for direct download from the United State Geological Survey (USGS) Earth Explorer database (`https://earthexplorer.usgs.gov/`). The eMODIS products includes either 7- or 10-day composite datasets with it's native highest spatial resolution of $250 \times 250\,m$ pixels size. The eMODIS NDVI V6 products provide NDVI datasets over entire world. For this study, the 10-day intervals products are download from the USGS website for the period 2003 - 2018 at three years interval, i.e., 2003, 2006, 2009, 2012, 2015, and 2018. The month of December is selected as it comes after the short-rainy season of September - November, therefore potentially making it more suitable for identifying NDVI changes (Awange et al., 2019a). A total of 18 images are downloaded for December, i.e., 3 images for each year, with the temporal duration of the images being 10 or 11 days, i.e., 1st-10th, 11th-20th and 21st-31st for the evaluated month (December). The imagery itself have coarse spatial resolution that encompasses the entire area of the African continent. These products are regarded as high temporal resolution, therefore, might be a suitable products for identifying areas of spatio-temporal changes in vegetation coverage (Chen et al., 2016). The focus of this study is on the vegetation of the catchment area for the entire LVB, therefore, the areal extent of the study is the lakes's surrounding areas (land area with vegetation cover) resulting in output masking the lake's surface. A subset image created for 2018 MODIS NDVI data using the shapefile of the LVB. All the rest of MODIS imagery are clipped using 2018 subset image. During the sub-setting of the images, a snap to pixel technique is used to make sure every pixel for all year represent the same geographical location for capturing genuine changes in NDVI values for the evaluated years.

2.2.2. *Google Earth Pro*

Google Earth Pro (GEP) is one of the online platform that uses base images with the option that provides time series image analysis through image slider tool (Saleem & Awange, 2019).

This platform provides high to medium resolution satellite images, for instance IKONOS and Landsat, respectively, over the world with variations from one region to another. For this study, the freely available historical Landsat images from GEP are used to visually analyse further (Section 3.4 and Figure 7) the identified NDVI hotspots where vegetation changes occur (see Figure 6). The triggers for these changes could be factors that include anthropogenic activities, e.g., urbanisation, forest and agriculture areas clearing. Furthermore, such visual analysis aid in showing the extent of anthropogenic contributions to vegetation changes.

2.2.3. GSFC Mascons

Mass-concentration (mascon) grids are monitored by the Gravity Recovery and Climate Experiment (GRACE) dual-satellite. The GSFC mascon estimation is processed by a general approach that it models the best-fit trend and annual time-variable gravity signals (Sabaka et al., 2008; Luthcke et al., 2013). It is worth mentioning that although the GSFC solution is comprised of 41,168, 1 arc-degree mascon cells, the original spatial resolution within a region is still 300 km. This means the time series of GSFC for each mascon within the same constraint region (e.g., basins) is highly correlated to the near mascons. In this study, GSFC mascon is used to monitor the equivalent water changes for every month, and compared to rainfall and vegetation changes.

2.2.4. CHIRPS Rainfall

Climate Hazards Group InfraRed Precipitation with Station data (CHIRPS) is a rainfall product that was developed to support the United States Agency for International Development Famine Early Warning Systems Network (FEWS NET) (Funk et al., 2015a). It merges satellite and in-situ observations to perform high spatial ($0.05° \times 0.05°$) resolution and monthly temporal results , e.g., National Oceanic and Atmospheric Administration's (NOAA's) Rainfall Estimate (REF2) (Love et al. , 2004), African Rainfall Climatology (Novella and Thiaw , 2013), CHPclim dataset (Funk et al., 2015b) and gauge products (Funk et al., 2015a). Generally, climate change is inferred from climatology data that spans more than 30 years. Given that CHIRPS data are available for 34 years, undertaking a PCA analysis on it can indicate the impacts of climate change through the analysis of its time series. When this is compared with the epochs of vegetation, one can infer on the impacts of climate change/variability on vegetation. The data is available on https://earlywarning.usgs.gov/fews/datadownloads/Global/CHIRPS.

Table 1: A summary of data employed in this study.

Description	Sensor	Time-line	Purpose	Data Source
NDVI	MODIS	Dec. 2003-2018	Vegetation changes	https://earthexplorer.usgs.gov/
Google Earth Pro	Landsat	Dec. 2003-2016	Anthropogenic impacts	Application-based
GSFC Mascons	GRACE	January 2003 – July 2016	Water altimetry changes	https://ccar.colorado.edu/grace/gsfc.html
Infrared rainfall data	CHIRPS	1984-2018	Impacts of climate change	http://chg.geog.ucsb.edu/data/chirps/

2.3. Methods

NDVI change maps are created for inter-annual and intra-annual variations for the 2003, 2006, 2009, 2012, 2015, and 2018 MODIS imagery datasets to identify zones of the catchment area that have undergone extensive decline in vegetation coverage. Principal Component Analysis (PCA) is computed on rainfall data to determine if any reduction in vegetation is climate-driven with help of the change maps generated from NDVI data. Google Earth Pro (GEP) imagery from the time of vegetation decrease for each hotspot is obtained to visualise if the decline is anthropogenically-driven. There are large amount of variance in NDVI values among the evaluated years, what can be partly attributed to the low spatial resolution ($250 \times 250\,m$ pixels size) of MODIS imagery. However, high temporal resolution of the data permit a valid comparison over time for the NDVI value changes. An NDVI threshold of $>$ 0.2 is used to determine whether a pixel is considered vegetation or non-vegetation (e.g., Pu et al., 2008; Duarte et al., 2018), and the total area of vegetation and non-vegetation for each year then determined by generating binary dataset for each year using ArcGIS environment. This section elaborates on the image-processing procedures used, including; fishnet creation, binary outputs, standardised anomaly, image difference. A structure chart of the methodology is presented in Figure 2.

2.3.1. Pre-processing

All 18 of the MODIS images are clipped to the extent of the basin outside of the lake prior to further processing. NDVI values $>$ 0.2 are extracted to create binary outputs depicting vegetation and non-vegetation pixels. The same threshold value was used in Pu et al. (2008); Duarte et al. (2018) as a means of representing shrubs and meadows. The NDVI statistics of the images are further normalised to provide the exact NDVI values of all vegetation pixels determined from the binary output, as well as categorising all non-vegetation pixels ≥ 0.2 as a '0' value.

A fishnet of points is then created for each pixel in the study area (over 2.6 million; 250 m x 250 m pixels). Within the fishnet dataset, the NDVI values for each pixel is extracted from all images and added to their respective points. The pixel mean NDVI value (i.e., the mean was used for original products for 7 or 10 days interval) for each year (2003, 2006, 2009, 2012, 2015, and 2018) is calculated from the three NDVI values of the original datasets of each year. The overall mean NDVI value of those years is then obtained from these outputs, i.e., the pixel mean for all years is then calculated using the pixel mean values for each year, which in turn allows the overall mean NDVI values to be extracted. Using the pixel mean value of each year, new rasters are derived depicting vegetation and non-vegetation areas using the NDVI threshold of > 0.2.

2.3.2. Anomaly calculations

Annual anomalies are computed with respect to the mean change of each pixel. These values are utilised to demonstrate the extent of changes in NDVI of the basin. Two approaches are used to present this; (i) the inter-annual, which highlight short-term 3-year annual trends for NDVI differences, i.e., 2003-2006, 2006-2009 etc., and (ii), the intra-annual maps that present short and long-term trends demonstrating the degree of NDVI difference for each of the years in relation to 2003 (which is set as the base year).

2.3.3. Hotspot significance maps

The significance of the mean annual changes of NDVI P-value for each pixel is the determining factor in the identification of a "hotspot" signifying reduction in vegetation coverage. Vegetation decreases are indicated for Z-values < 0, with the significance of the trends of vegetation changes indicated by P-values < 0.05. P and Z values are calculated for all pixels in the study area where any pixel that fulfils both criteria is interpreted as decreasing at 95% confidence.

2.3.4. Principal Component Analysis (PCA)

Principal component analysis (PCA) is a technique for reducing the dimensionality of datasets, increasing interpretability but at the same time minimizing information loss(Awange et al., 2020). It is useful for identifying variance in hydrometeorological parameters Dyer (1975); Awange et al. (2011, 2014, 2016, 2019a). In this study, it is employed to analyse gridded

CHIRPS rainfall variation throughout the catchment area for the 1984-2018 period in order to infer the impacts of climate change on vegetation. As NDVI values are a measure of vegetation greenness, higher NDVI values are dependent on higher water content (Foody , 2003), eutrophication (especially around the lake perimeter, e.g., Coladello et al., (2020)), the vegetation type (e.g., (Omute et al., 2012)), density and height which translated in high NDVI values. Also, in such spatial resolution (250 m) mixed pixels significantly affect the NDVI values on the one hand while on the other hand, the meteorological conditions in the previous days of the selected MODIS images can affect the NDVI values. The patterns determined from the PCA analysis can determine whether the reduction in NDVI values from the 'hotspots' derived from the MODIS imagery processing are climate-driven through the analysis of rainfall variability (e.g., Awange et al., 2016, 2019a) and comparing with changes in NDVI (e.g., Omute et al., 2012).

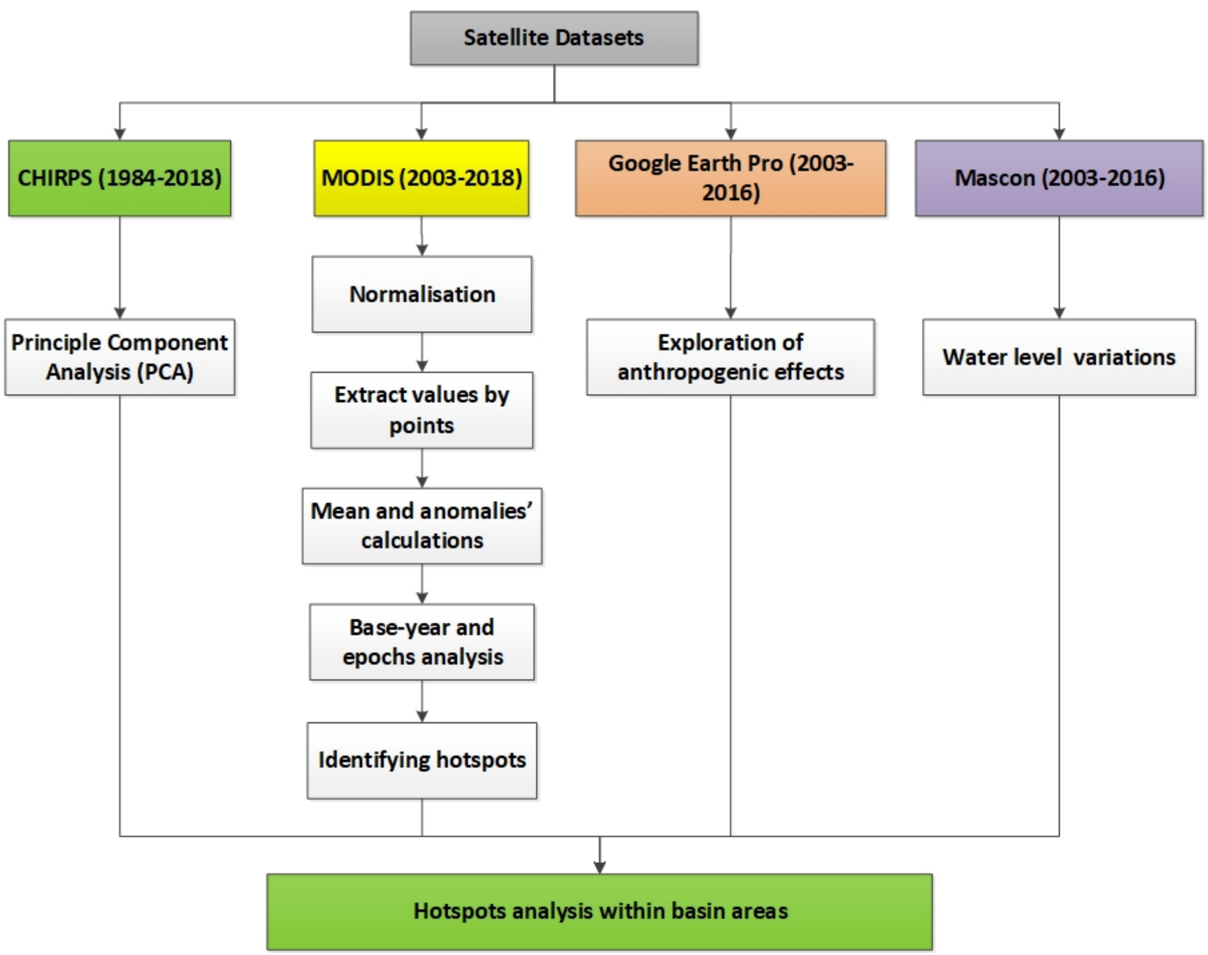

Figure 2: Workflow for the investigation.

3. Results and discussion

3.1. Vegetation analysis within LVB

The lower mean NDVI values for December 2006 and 2018 (Figure 3a) can be largely attributed to the lower than average rainfalls in Eastern Africa, which were caused by the occurrence of La Ñina events in 2006 and 2016-2017 respectively (Hoell et al., 2017; Setimela et al., 2018). Conversely, the higher mean NDVI value for December 2015 (Figure 3a) can be attributed to higher than average rainfalls from the occurrence of an El Ñino event in 2015-2016 (Setimela et al., 2018).

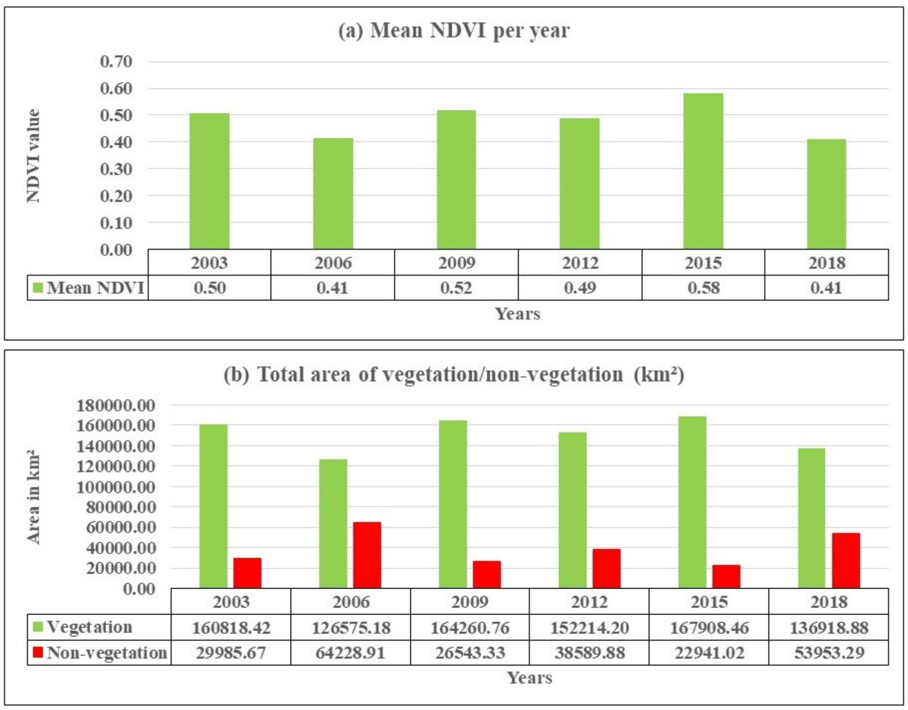

Figure 3: (a) Mean NDVI, and (b), Area of vegetation/non-vegetation using NDVI > 0.2 threshold.

3.1.1. *Epoch and base-year trend change maps*

As stated earlier (see Section 2.3.2), epoch and long-term trends of NDVI changes indicate the potential whereabouts of significant hotspots in the basin. The primary purpose of these maps is to identify areas in the LVB have undergone drastic transformations in overall vegetation greenness within its respective recorded period.

As the epoch maps highlight the short-term 3-year annual trends, it therefore can highlight the extent in the variation of NDVI values caused by extreme weather events. The 2003-2006 and 2015-2018 maps (Figure 4a) display the magnitude of environmental impact caused by lower than average rainfall from their respective La Ñina events that were highlighted in Hoell et al. (2017); Setimela et al. (2018). Figure 4a demonstrates the capacity in which rainfall variations can have on the environment in the short-term. However, vegetation that has yet to be subjected to significant human interference has the capacity to replenish when annual rainfall levels increase. This is displayed in the 2006-2009 (Figure 4a), which occurred after the La Ñina event of 2006 as well as the 2012-2015 period (Figure 4a, which occurred during the El Ñino event of 2015-2016. The decreases of NDVI values are more widespread and of greater magnitude. In 2003-2006 the impact is generally more profound west of the lake. Significant clusters of reduced NDVI values have been identified in the south-west of the catchment area (Burundi), central to the western side of the lake (Tanzania), north-west of the catchment area (Uganda) and Central Rwanda. East of LVB, there is a large general decrease of NDVI spread across Kenya, which sprawls across into the Tanzanian border and continues nearby to the southern border of the lake.

In the 2015-2018 period, the impact is even more extreme. There are additional areas that have undergone significant NDVI decreases; namely along the northern boundary of the lake as well as more extensively east of the lake across Kenya and Tanzania. However, it must be stated that the extremity of the reduction is harnessed from the contrasting extreme weather events that occurred in 2015 and 2018. As stated in Section 3.1, higher than average rainfall occurred in the Lake Victoria region due to an El Ñino event in 2015-2016, whereas lower than average rainfall occurred due to a La Ñina event in 2016-2017 (Setimela et al., 2018). These extreme weather events would be the primary contributor as to why NDVI is higher than normal for 2015, and lower than normal for 2018. This means that when computing the difference in the pixel anomalies inter-annually for 2015-2018, the result would indicate widespread NDVI decrease.

The base-year map (Figure 4b) highlights the long-term trends for NDVI changes for all years from 2003. In a similar vein to the outputs for the epoch maps (Figure 4a), the western side of the basin is substantially more impacted. Within the 15-year time-span; south-western Uganda, north-western Tanzania, central and eastern Rwanda as well as northern Burundi have all been inflicted in this negative trend. East of the lake has also undergone some impact, particularly in an area in south-western Kenya. However, the long-term trend indicates that most of the primary hotspots occur west of the lake, see more details in Section 3.1.2.

3.1.2. Identification of significant hotspots

The next step is to determine the whereabouts of statistically significant hotspots that indicate a long-term trend in vegetation decline. The criteria for identifying pixels that would formulate the hotspots are $Z \leq$ -2 and $P < 0.05$, indicating significant decrease at 95% confidence. All pixels meeting this criteria are extracted from their respective datasets. All pixels that represent both criteria could potentially be located within clusters of similar pixels. There are such pixels located widespread in the study area, however, the purpose is to identify more aggregations, i.e., areas, in which the separation of neighbouring pixels is no greater than 30 km. Due to the large size of the study area, it is understood that using a larger distance threshold could provide a more sustainable output in terms of the number of clusters that will result.

That resultant output when utilising the 30-km separation threshold are 8 significant hotspots (Figure 4c); 5 of which were in Uganda, and 1 each for Kenya, Tanzania and Rwanda respectively. With Uganda containing the most hotspots, those findings correlate with the long-term trends analysed in Section 3.1.1, in which vegetation located north-west of Lake Victoria was found to have undergone the largest areal decrease in NDVI from 2003-2018. Evidently, parts of the study area that were subjected to short-term vegetation changes were not deemed significant enough in the P and Z outputs in Figure (4c) to be deemed a hotspot.

The results show that there is some correlation between the NDVI hotspots deduced in this investigation and the hotspots discovered in Awange et al. (2019a) that demonstrated a significant decrease in the surface area of Lake Victoria itself. That study concluded that Winam gulf (Kisii, Kenya), Emin Pasha gulf (Katoro, Tanzania), Mwanza gulf and Birinzi

(Kampala & Masaka, Uganda) were the hotspots. Each of these places has expanded their urban environments to various extents since 2003, whilst also showing signs of deforestation and clearing to enable the provision of agriculture and other rural industry. The assumption can be made that this outwards urban expansion has not only reduced all vegetation characteristics but has also necessitated the extraction of nearby freshwater that Lake Victoria provides for these areas.

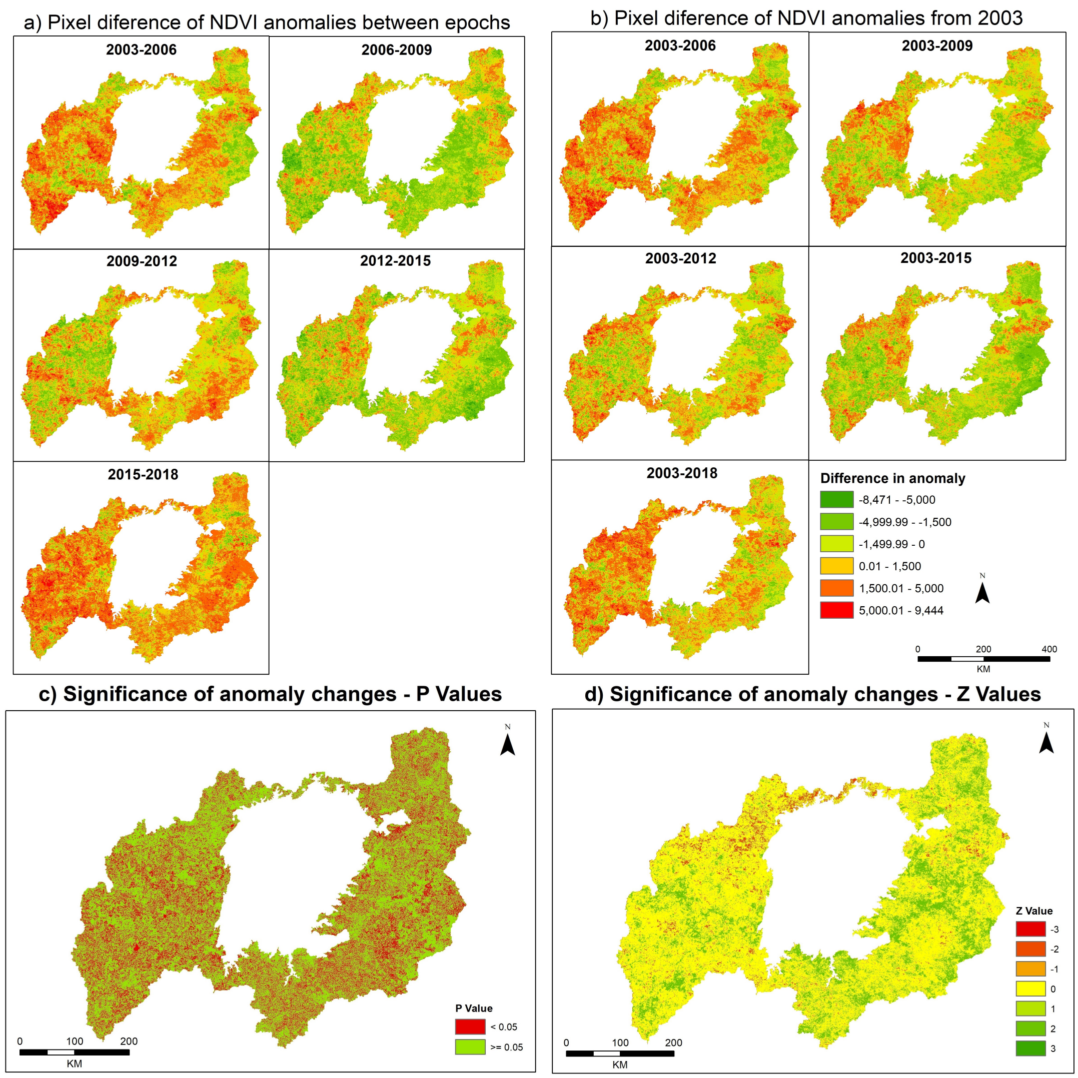

Figure 4: (a) Short-term three-year epoch differences in NDVI, (b) long-term NDVI trends from 2003, (c), significance of anomaly changes using maps depicting P values, and (d), significance of anomaly changes using maps depicting Z values.

3.2. Rainfall variability within LVB

For the 1984-2018 period, a PCA analysis is performed on the rainfall parameters within LVB. Figure 5 shows the principal components (PC; time series) and the empirical orthogonal functions (EOF; spatial maps) both of which have to be interpreted together to understand rainfall variability within the LVB. Both PCs and EOFs account for the total variation in the rainfall (Dyer , 1975). The results of the PCA, where PC1 (accounting for 75.2% of the overall variance in rainfall) depicts the dominant seasonal rainfall superpositioned with the annual signal, PC2 (19.1%) shows annual rainfall variation, while PC3 (5.6%) shows extreme rainfall events (i.e., those associated with El Ñino and La Ñina)), are consistent, e.g., with the results of Awange et al. (2013) who found four modes over the basin for the period 2003-2013. For instance, Awange et al. (2013)'s PC1 (representing 63% of total variance of the rainfall) showed a superposition of the annual and seasonal variabilities while PC2 (13%) related to the annual variation and PC3 showed a summation of interannual changes and a linear trend over the basin. The first three EOF modes in the present study are identical to those of Awange et al. (2013). Other similar findings are presented, e.g., in (e.g., Khaki & Awange , 2019; Awange et al., 2019a).

Identifying if there are climatic drivers in the formation of NDVI hotspots is accomplished through analysing the variation trends derived from the PCA output. In general, overall rainfall decreased throughout the Lake Victoria basin, in some places by as high as 250 millimetres, such as along the western boundary of the lake and along the south-western boundary of the study area within Burundi. Seasonality caused its most profound rainfall decrease along the southern extremities of the study area. The decrease became gradually less profound progressively north from the southern extent. The north-eastern corner overlapping Kenya and Uganda recorded increased rainfall due to seasonal variations. Extreme weather events result in horizontal contrast with increased rainfall recorded over most of the western half of the study area and decreased rainfall over most of the eastern half.

For the NDVI hotspot identified in Kisii, Kenya the only rainfall variable that could have had any effect in the long-term reduction in NDVI is the La Ñina extreme weather events. However, as that only accounts for 5.6% of rainfall variation, it is safe to assume that the hotspot is the result of a non-climatic driver. For all the Ugandan hotspots, PCA does not provide any meaningful indicator for climate contributing to its formation. Conversely, the total rainfall and seasonality PCs indicate some possibility that they contribute to the formation of the Kigali (Rwanda) and Katoro (Tanzania) hotspots. These PCs account for approximately 94.3% of rainfall variance, which is reason enough to suggest that climatic impact could be meaningful.

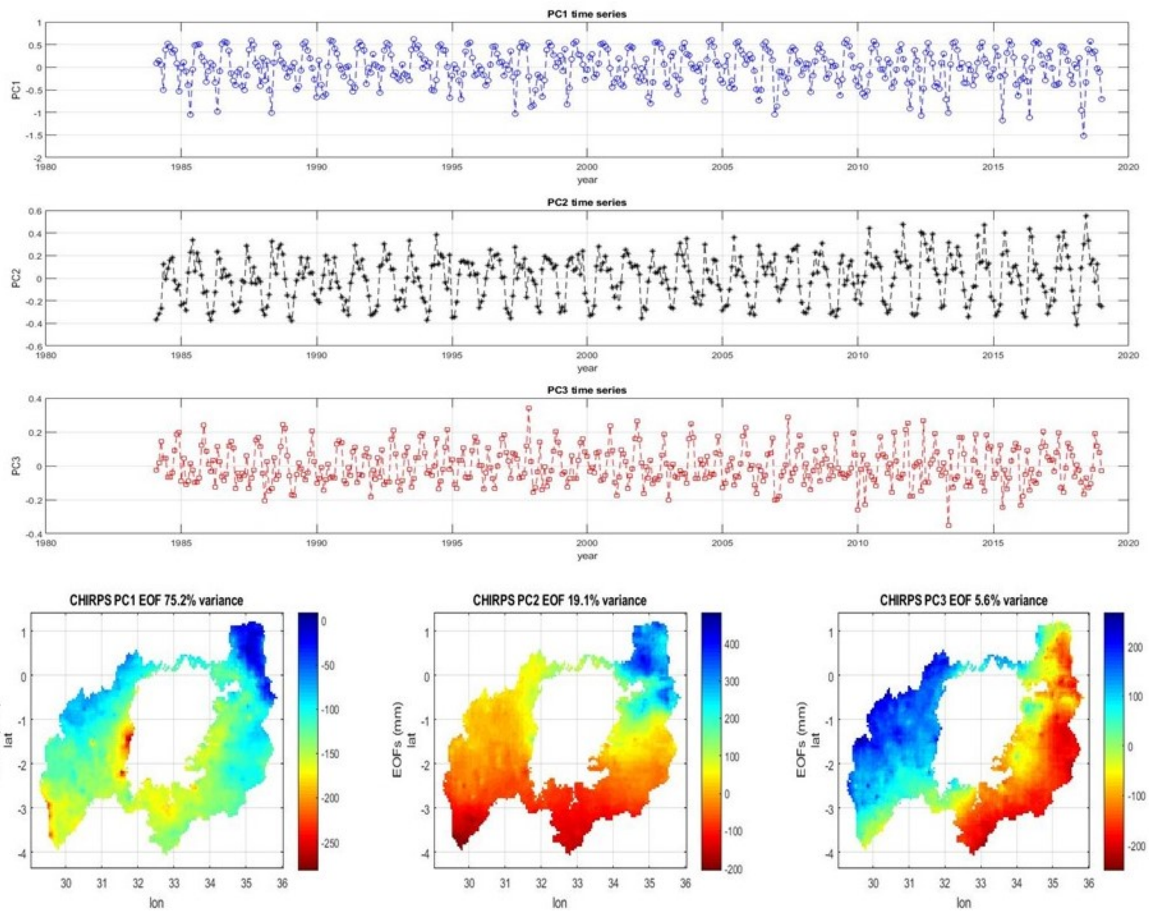

Figure 5: PCA analysis (a) Timeseries of PCA components, and (b), spatial pattern of components.

3.3. Total Water Storage changes within the hotspots

Annual total water storage (TWS; surface, groundwater, soil moisture and vegetation) changes have been obtained for all Gravity Recovery and Climate Experiment (GRACE) Mass Concentration (mascon) grids where hotspots lie (see Figure 6). The La Ñina event in 2006 presents a decrease in TWS by approximately 2 gigatons for all mascons. In contrast, the El Ñino event in 2015-2016 presented an annual increase of approximately 3-4 gigatons for all mascons.

However, a short-coming in these assessments is their time-span. Analysis of NDVI changes occurred every three years from 2003-2018 while the mascon analysis occurs from January 2003 – July 2016. The major detriment for that is that a La Ñina event occurred in 2016-2017, resulting in lower rainfall for Eastern Africa. The effects that this had on TWS changes is not recorded. As December 2018 is the final period for NDVI analysis, the short-term and long-term effects of the La Ñina event is displayed in Section 3.1.1. With the missing TWS change data, it makes it difficult to determine if rainfall variables are a major driver in the formation of the NDVI hotspots.

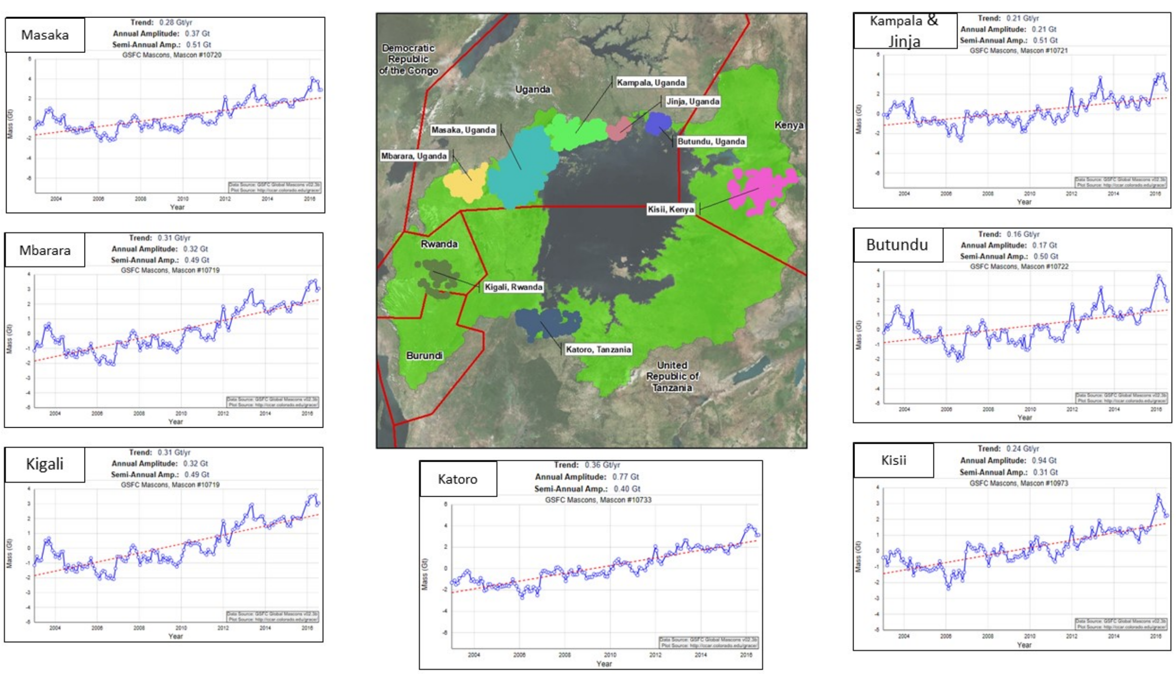

Figure 6: Gravity Recovery and Climate Experiment (GRACE) Mass Concentration mascon analysis of the total water storage changes within the NDVI hotspots.

3.4. Google Earth Pro imagery

The identified NDVI hotspots from MODIS data is assessed further using the satellite imagery from GEP at different time-scales to provide insight into the extent of the anthropogenic impacts. From the analysis it is evident that for the Ugandan hotspots of Jinja, Kampala, Masaka and Mbarara, that outward urban expansion is the primary contributor for the long-term NDVI decline. The same conclusion can be drawn for the Rwandan and Kenyan hotspots also. The Katoro (Tanzania) hotspot can also be seen to have undergone urban expansion, but to a lesser extent. The Ugandan hotspot of Butundu is not necessarily derived from urbanisation, but it was still caused by anthropogenic activities, as it appears that large-scale deforestation and clearing occurred in the region for widespread agricultural practices to begin.

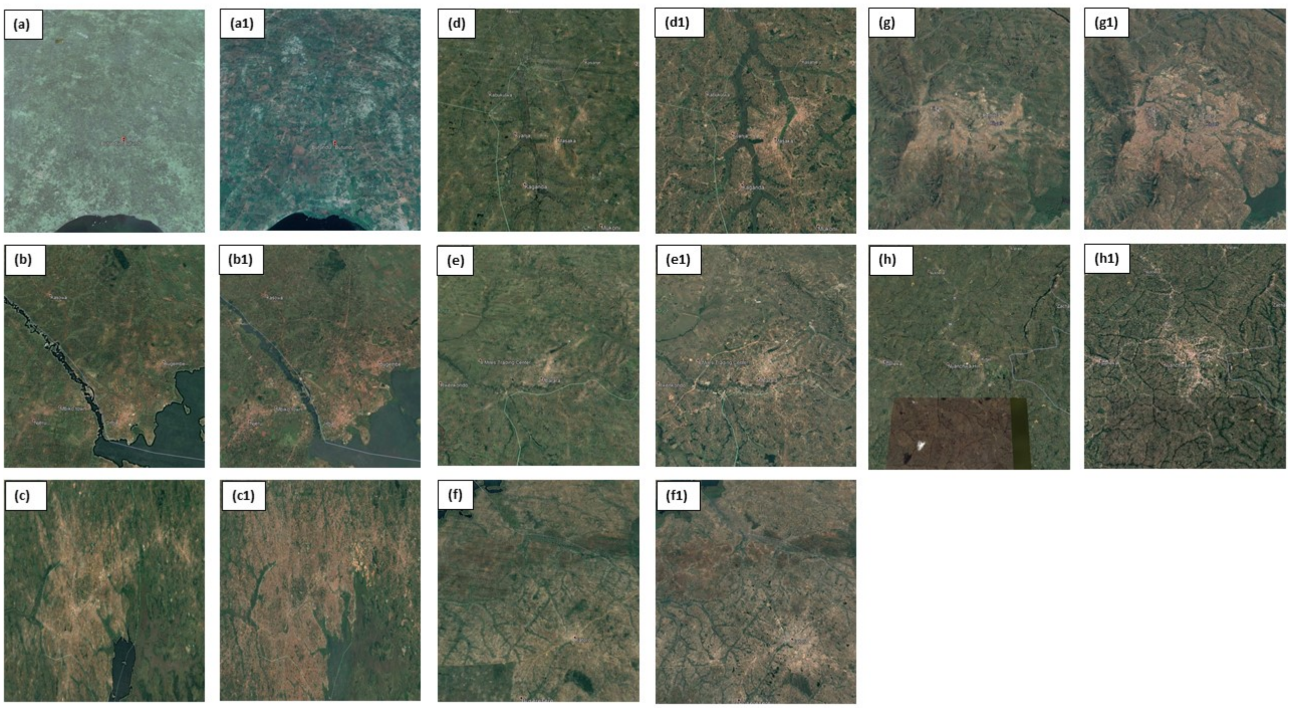

Figure 7: Google Earth Pro imagery with Landsat images as base map (a) Butundu, Uganda 2004 and (a1) Butundu, Uganda 2017; (b) Jinja, Uganda 2003 and (b1) Jinja, Uganda 2016; (c) Kampala, Uganda 2003 and (c1) Kampala, Uganda 2016; (d) Masaka, Uganda 2003 and (d1) Masaka, Uganda 2016; (e) Mbarara, Uganda 2003 and (e1) Mbarara, Uganda 2016; (f) Katoro, Tanzania 2003 and (f1) Katoro, Tanzania 2016; (g) Kigali, Rwanda 2003 and (g1) Kigali, Rwanda 2016; (h) Kisii, Kenya 2003 and (h1) Kisii, Kenya 2018.

4. Conclusion

Following a recent study that indicated reduction of Lake Victoria's surface over the period 1984-2018, this contribution aimed at investigating changes in vegetation cover over the Lake Vectorial Basin (LVB) over the period 2003-2018. To achieve this, the study employed MODIS (Moderate Resolution Imaging Spectroradiometer), Google Earth Pro, CHIRPS (Climate Hazards Group InfraRed Precipitation with station data) precipitation data, Google Earth Pro imagery, Gravity Recovery and Climate Experiment (GRACE)-based Mascon's water storage products, and the statistical method of Principal Component Analysis (PCA). The assumption, here, is that changes in vegetation within LVB is related to the lake's physical dynamics and as such, understanding vegetation changes within the basin and identifying the hotspots where they occur could be essential to the overall management of the lake. The results show that the vegetation within the LVB experienced temporal variations throughout the study period (2003-2018). Specifically, the study found that:

1. Long-term vegetational changes within LVB over the period 2003-2018 were primarily anthropologically driven, with urbanization expanding at the expense of vegetation as seen from the Google Earth Pro imagery.
2. Eight "hotspots" (i.e., areas with significant vegetational changes) in total were identified over LVB: 5 in Uganda, and one each in Kenya (Kisii), Kigali (Rwanda) and Tanzania. Other than the Rwandan and Tanzanian hotspots where climate variability impacts were visible, there is no meaningful evidence presented from the rainfall and Mascon's TWS analysis to suggest that anything other than human processes is causing long-term changes in vegetation characteristics over the other hotspots.
3. Out of all the countries within the LVB, it can be said that Uganda has undergone the most profound urbanisation processes since 2003, largely due to the expansion of its major cities such as Kampala, Masaka and Jinja that were identified as hotspots. Small-scale urban expansion also occurred in the Butundu, Mbarara and Katoro cities that do not serve as major urban hubs, but instead service agricultural and industrial practices. The expansion of these regional practices can be attributed to why they have been identified as vegetation hotspots, as clearing of land is required to facilitate these practices.

Understanding the locations of vegetational changes is most profound, as well as the driving forces associated with such changes, in that it provides critical information to major stakeholders regarding future environmental management, policies and planning. Management of Lake Victoria and its basin, therefore, would benefit from such analysis presented in this work.

5. Acknowledgment

A. Saleem is grateful for the opportunity offered to him by Curtin University, School of Earth and Planetary Sciences to undertake his postdoctoral studies. J.L. Awange would like to thank the financial support of the Alexander von Humboldt Foundation that supported his time at Karlsruhe Institute of Technology (Germany). He is grateful to the good working atmosphere provided by his hosts Prof and Hansjörg Kutterer and Prof Bernhard Heck.

References

References

Agutu, N. O., Awange, J. L., Ndehedehe, C., & Mwaniki, M. (2020). Consistency of agricultural drought characterization over Upper Greater Horn of Africa (1982–2013): Topographical, gauge density, and model forcing influence. Science of The Total Environment, 709, 135149.

Awange JL, Fleming KM, Kuhn M, Featherstone WE, Anjasmara I, Heck B (2011) On the suitability of the 4o x 4o GRACE mascon solutions for remote sensing Australian hydrology. Remote Sensing of Environment 115: 864-875, doi: 10.1016/j.rse.2010.11.014.

Awange JL, Forootan E, Kuhn M, Kusche J, Heck B (2014) Water storage changes and climate variability within the Nile Basin between 2002 and 2011. Advances in Water Resources 73:1-25, doi: 10.1016/j.advwatres.2014.06.010.

Awange JL, Anyah R, Agola N, Forootan E, Omondi P (2013) Potential impacts of climate and environmental change on the stored water of Lake Victoria Basin and economic implications. Water Resources Research 49: 8160 – 8173, IF 3.149, doi: 10.1002/2013WR014350

Awange JL, Khandu, Forootan E., Schumacher M., Heck B (2016) Exploring hydro-meteorological drought patterns over the Greater Horn of Africa (1979-2014) using remote sensing and reanalysis products. Advances in Water Resources 94: 45-59, doi:10.1016/j.advwatres.2016.04.005.

Awange, J. L., Saleem, A., Sukhadiya, R. M., Ouma, Y. O., & Kexiang, H. (2019a). Physical dynamics of Lake Victoria over the past 34 years (1984–2018): Is the lake dying?. Science of The Total Environment, 658, 199-218.

Awange, J. L., Hu, K. X., & Khaki, M. (2019b). The newly merged satellite remotely sensed, gauge and reanalysis-based Multi-Source Weighted-Ensemble Precipitation: Evaluation over Australia and Africa (1981–2016). Science of The Total Environment, 670, 448-465.

Awange JL, Palancz B and Völgyesi L (2020) Hybrid Imaging and Visualization. Employing Machine Learning with Mathematica - Python. Springer Nature International, Berlin.

Awange, J. L., Sharifi, M. A., Ogonda, G., Wickert, J., Grafarend, E. W., & Omulo, M. A. (2008). The falling Lake Victoria water level: GRACE, TRIMM and CHAMP satellite analysis of the lake basin. Water Resources Management, 22(7), 775-796.

Awange, J. L., & Ong'ang'a, O. (2005). Lake Victoria. Ecology, Resources and Environment. Springer-Verlag, Berlin. New York.

Baeriswyl, P.-A., & Rebetez, M. (1997). Regionalization of precipitation in Switzerland by means of principal component analysis. Theoretical and Applied Climatology, 58(1-2), 31-41.

Baldwin, A. H., Egnotovich, M. S., & Clarke, E. (2001). Hydrologic change and vegetation of tidal freshwater marshes: field, greenhouse, and seed-bank experiments. Wetlands, 21(4), 519-531.

Chen, Y., Song, X., Wang, S., Huang, J., & Mansaray, L. R. (2016). Impacts of spatial heterogeneity on crop area mapping in Canada using MODIS data. ISPRS Journal of Photogrammetry and Remote Sensing, 119, 451-461.

Cheruiyot, E., Mito, C., Menenti, M., Gorte, B., Koenders, R., & Akdim, N. (2014). Evaluating MERIS-based aquatic vegetation mapping in Lake Victoria. Remote Sensing, 6(8), 7762-7782.

Detsch, F., Otte, I., Appelhans, T., Hemp, A., & Nauss, T. (2016). Seasonal and long-term vegetation dynamics from 1-km GIMMS-based NDVI time series at Mt. Kilimanjaro, Tanzania. Remote Sensing of Environment, 178, 70-83.

Duarte, L., Teodoro, A. C., Monteiro, A. T., Cunha, M., & Gonçalves, H. (2018). QPhenoMetrics: An open source software application to assess vegetation phenology metrics. Computers and Electronics in Agriculture, 148, 82-94.

Dinku, T., Funk, C., Peterson, P., Maidment, R., Tadesse, T., Gadain, H., & Ceccato, P. (2018). Validation of the CHIRPS satellite rainfall estimates over eastern Africa. Quarterly Journal of the Royal Meteorological Society, 144, 292-312.

Dyer, T. G. (1975). The assignment of rainfall stations into homogeneous groups: an application of principal component analysis. Quarterly Journal of the Royal Meteorological Society, 101(430), 1005-1013.

Foody, G. M. (2003). Geographical weighting as a further refinement to regression modelling: An example focused on the NDVI–rainfall relationship. Remote sensing of Environment, 88(3), 283-293.

Funk, C., Peterson, P., Landsfeld, M., Pedreros, D., Verdin, J., Shukla, S., Husak, G., Rowland, J., Harrison, L., Hoell, A. and Michaelsen, A. (2015a), The climate hazards infrared precipitation with stations—a new environmental record for monitoring extremes, Scientific Data, 2, 150066, doi:10.1038/sdata.2015.66 2015.

Funk, C., Verdin, A., Michaelsen, J., Peterson, P., Pedreros, D. and Husak, G. (2015b), A global satellite assisted precipitation climatology, Earth System Science Data Discuss, 7, 1-13, doi:10.5194/essd-7-275-2015.

Haroon, M. A., & Rasul, G. (2009). Principal component analysis of summer rainfall and outgoing long-wave radiation over Pakistan. Pakistan Journal of Meteorology, 5(10).

Hill, N. M., Keddy, P. A., & Wisheu, I. C. (1998). A hydrological model for predicting the effects of dams on the shoreline vegetation of lakes and reservoirs. Environmental management, 22(5), 723-736.

Hoell, A., Funk, C., Zinke, J., & Harrison, L. (2017). Modulation of the southern Africa precipitation response to the El Niño Southern Oscillation by the subtropical Indian Ocean dipole. Climate dynamics, 48(7-8), 2529-2540.

Hu, K., Awange, J. L., Forootan, E., Goncalves, R. M., & Fleming, K. (2017). Hydrogeological characterisation of groundwater over Brazil using remotely sensed and model products. Science of the Total Environment, 599, 372-386, doi:10.1016/j.scitotenv.2017.04.188.

Hudon, C. (1997). Impact of water level fluctuations on St. Lawrence River aquatic vegetation. Canadian Journal of Fisheries and Aquatic Sciences, 54(12), 2853-2865.

Jeppesen, E., Søndergaard, M., Lauridsen, T. L., Davidson, T. A., Liu, Z., Mazzeo, N., & Starling, F. (2012). Biomanipulation as a restoration tool to combat eutrophication: recent advances and future challenges. In Advances in ecological research (Vol. 47, pp. 411-488). Academic Press.

Jolliffe, T. I., & Cadima, J. (2016). Principal component analysis: a review and recent developments. Philos Trans A Math Phys Eng Sci., 374(2065), doi:10.1098/rsta.2015.0202.

Khaki, M., & Awange, J. (2019). Improved remotely sensed satellite products for studying Lake Victoria's water storage changes. Science of the Total Environment, 652, 915-926.

Kizza, M., Rodhe, A., Xu, C. Y., Ntale, H. K., & Halldin, S. (2009). Temporal rainfall variability in the Lake Victoria Basin in East Africa during the twentieth century. Theoretical and applied climatology, 98(1-2), 119-135.

Coladello, L., Galo, M., Ivanová, I., Awange, J., & Shimabukuro, M., (2020) Macrophytes' abundance changes in eutrophicated tropical reservoirs exemplified by Salto Grande (Brazil): Trends and temporal analysis exploiting Landsat remotely sensed data. Applied Geography. In Press.

Li, Z., & Kafatos, M. (2000). Interannual variability of vegetation in the United States and its relation to El Ñino/Southern Oscillation. Remote Sensing of Environment, 71(3), 239-247.

Love, T. B., Kumar, V., Xie, P.& Thiaw, W. (2004), A 20-year daily Africa precipitation climatology using satellite and gauge data, Seattle, In Proceedings of the 84th AMS Annual Meeting, vol. Conference on Applied Climatology.

Luthcke, S. B., Sabaka, T. J., Loomis, B. D., Arendt, A. A., McCarthy, J. J., & Camp, J. (2013). Antarctica, Greenland and Gulf of Alaska land-ice evolution from an iterated GRACE global mascon solution.

Mati, B. M., Mutie, S., Gadain, H., Home, P., & Mtalo, F. (2008). Impacts of land-use/cover changes on the hydrology of the transboundary Mara River, Kenya/Tanzania. Lakes & Reservoirs: Research & Management, 13(2), 169-177.

New, T., & Xie, Z. (2008). Impacts of large dams on riparian vegetation: applying global experience to the case of China's Three Gorges Dam. Biodiversity and Conservation, 17(13), 3149-3163.

Nicholson, S. E., Davenport, M. L., & Malo, A. R. (1990). A comparison of the vegetation response to rainfall in the Sahel and East Africa, using normalized difference vegetation index from NOAA AVHRR. Climatic change, 17(2-3), 209-241.

Nilsson, C., & Berggren, K. (2000). Alterations of riparian ecosystems caused by river regulation: Dam operations have caused global-scale ecological changes in riparian ecosystems. How to protect river environments and human needs of rivers remains one of the most important questions of our time. BioScience, 50(9), 783-792.

Novella, N.S. and Thiaw, W.M. (2013), African rainfall climatology version 2 for famine early warning systems, Journal of Applied Meteorology and Climatology, 52, 588–606, doi:10.1175/JAMC-D-11-0238.1.

Okotto-Okotto, J., Raburu, P. O., Obiero, K. O., Obwoyere, G. O., Mironga, J. M., Okotto, L. G., & Raburu, E. A. (2018). Spatio-temporal impacts of Lake Victoria water level recession on the fringing Nyando Wetland, Kenya. Wetlands, 38(6), 1107-1119.

Omute, P., Corner, R., & Awange, J. L. (2012). The use of NDVI and its derivatives for monitoring Lake Victoria's water level and drought conditions. Water resources management, 26(6), 1591-1613.

Park, S., Kang, D., Yoo, C., Im, J., & Lee, M. I. (2020). Recent ENSO influence on East African drought during rainy seasons through the synergistic use of satellite and reanalysis data. ISPRS Journal of Photogrammetry and Remote Sensing, 162, 17-26.

Plisnier, P. D., Serneels, S., & Lambin, E. F. (2000). Impact of ENSO on East African ecosystems: a multivariate analysis based on climate and remote sensing data. Global Ecology and Biogeography, 9(6), 481-497.

Preisendorfer, R. W. (1988). Introduction. In C. Mobley (Ed.), Principal Component Analysis in Meteorology and Oceanography (pp. 1-9). Elsevier, Amsterdam.

Pu, R., Gong, P., Tian, Y., Miao, X., Carruthers, R. I., & Anderson, G. L. (2008). Using classification and NDVI differencing methods for monitoring sparse vegetation coverage: a case study of saltcedar in Nevada, USA. International Journal of Remote Sensing, 29(14), 3987-4011.

Richard, Y., & Poccard, I. (1998). A statistical study of NDVI sensitivity to seasonal and interannual rainfall variations in Southern Africa. International Journal of Remote Sensing, 19(15), 2907-2920.

Sabaka, T. J., D. D. Rowlands, S. B. Luthcke, and J. P. Boy (2010), Improving global mass flux solutions from GRACE through forward modeling and continuous time-correlation, J. Geophys. Res., doi:10.1029/2010JB007533.

Saleem, A., & Awange, J. L. (2019). Coastline shift analysis in data deficient regions: Exploiting the high spatio-temporal resolution Sentinel-2 products. Catena, 179, 6-19.

Sand-Jensen, K., Riis, T., Vestergaard, O., & Larsen, S. E. (2000). Macrophyte decline in Danish lakes and streams over the past 100 years. Journal of Ecology, 88(6), 1030-1040.

Setimela, P., Gasura, E., Thierfelder, C., Zaman-Allah, M., Cairns, J. E., & Boddupalli, P. M. (2018). When the going gets tough: Performance of stress tolerant maize during the 2015/16 (El Niño) and 2016/17 (La Niña) season in southern Africa. Agriculture, ecosystems & environment, 268, 79-89.

Stathis, D., & Myronidis, D. (2009). Principal component analysis of precipitation in Thessaly region (Central Greece). Global NEST Journal, 11(4), 467-476.

Widmann, M., & Schär, C. (1997). A principal component and long-term trend analysis of daily precipitation in Switzerland. International Journal of Climatology, 17(12), 1333-1356.

Williams, C. A., & Hanan, N. P. (2011). ENSO and IOD teleconnections for African ecosystems: evidence of destructive interference between climate oscillations. Biogeosciences, 8(1), 27.

Zhang, Y., Jeppesen, E., Liu, X., Qin, B., Shi, K., Zhou, Y., & Deng, J. (2017). Global loss of aquatic vegetation in lakes. Earth-Science Reviews, 173, 259-265.

Zhao, J., Huang, S., Huang, Q., Wang, H., Leng, G., & Fang, W. (2020). Time-lagged response of vegetation dynamics to climatic and teleconnection factors. Catena, 189, 104474.